16 Physics of electroweak gauge bosons

Gauge bosons and gauge-boson pairs will be abundantly produced at the LHC. The large statistics and the high centre-of-mass energy will allow several precision measurements to be performed, which should improve significantly the precision achieved at present machines. Two examples of such measurements are discussed in this Chapter: the measurement of the W mass, which will benefit mainly from the large statistics, and the measurement of Triple Gauge Couplings (TGCs), which will benefit from both the large statistics and the high centre-of-mass energy.

In addition, measurements related to inclusive gauge boson production, gauge-boson pair production and gauge boson plus jet(s) production will be important to understand the underlying physics and measure the background for new particle searches. These issues are discussed in Section 15.7. Finally, Z production will be one of the main tools for the *in situ* calibration of the detector mass scale (Chapter 12).

16.1 Measurement of the *W* mass

At the time of the LHC start-up, the W mass will be known with a precision of about 30 MeV from measurements at LEP2 [16-1] and Tevatron [16-2]. The motivation to improve on such a precision is discussed briefly below. The W mass, which is one of the fundamental parameters of the Standard Model, is related to other parameters of the theory, *i.e.* the QED fine structure constant α, the Fermi constant G_F and the Weinberg angle $\sin\vartheta_W$, through the relation

$$m_W = \sqrt{\left(\frac{\pi\alpha}{G_F\sqrt{2}}\right)}\frac{1}{\sin\vartheta_W\sqrt{1-\Delta R}}$$

where ΔR accounts for the radiative corrections which amount to about 4%. The radiative corrections depend on the top mass as $\sim m_{top}^2$ and on the Higgs mass as $\sim log\ m_H$. Therefore, precise measurements of both the W mass and the top mass allow constraining the mass of the Standard Model Higgs boson or of the h boson of the MSSM. This constraint is relatively weak because of the logarithmic dependence of the radiative corrections on the Higgs mass.

Equivalent errors in the above relation arising from the uncertainties in the top mass and in the W mass imply that the precision on the top mass and on the W mass should be related by the expression

$$\Delta m_W \approx 0.7 \times 10^{-2}\Delta m_{top}$$

Since the top mass will be measured with an accuracy of about 2 GeV at the LHC (see Chapter 18), the W mass should be known with a precision of 15 MeV or better, so that it does not become the dominant error in the Higgs mass estimation. Such a precision is beyond the sensitivity of Tevatron and LEP2.

A study was performed to assess whether ATLAS will be able to measure the W mass to better than 20 MeV [16-3]. This measurement, which will be performed in the initial phase at low luminosity as the top mass measurement, would constrain the mass of the Higgs boson to better than 30%. When and if the Higgs boson will be found, such constraints would provide an im-

portant consistency check of the theory, and in particular of its scalar sector. Disentangling between the Standard Model and the MSSM might be possible, since the radiative corrections to the W mass are expected to be a few percent larger in the latter case.

The measurement of the W mass at hadron colliders is sensitive to many subtle effects which are difficult to predict before the experiment starts. However, based on the present knowledge of the ATLAS detector performance and on the experience from the Tevatron, it should be possible to make a reasonable estimate of the total uncertainty and of the main contributions to be expected. In turn, this will lead to requirements for the detector performance and theoretical inputs which are needed to achieve the desired precision. This is the aim of the study which is described in the next Sections.

16.1.1 The method

The measurement of the W mass at hadron colliders is performed in the leptonic channels. Since the longitudinal momentum of the neutrino cannot be measured, the transverse mass $m_T{}^W$ is used. This is calculated using the transverse momenta of the neutrino and of the charged lepton, ignoring the longitudinal momenta:

$$m_{\mathrm{T}}^{W} = \sqrt{2 p_{\mathrm{T}}^{l} p_{\mathrm{T}}^{\nu} (1 - \cos\Delta\phi)} \qquad 16\text{-}1$$

where $l = e, \mu$. The lepton transverse momentum $p_{\mathrm{T}}{}^l$ is measured, whereas the transverse momentum of the neutrino $p_{\mathrm{T}}{}^\nu$ is obtained from the transverse momentum of the lepton and the momentum $\bar{u}$ of the system recoiling against the W in the transverse plane (hereafter called 'the recoil'):

$$p_{\mathrm{T}}^{\nu} = -\left|\bar{p}_{\mathrm{T}}^{l} + \bar{u}\right|$$

The distribution of $m_{\mathrm{T}}{}^W$, and in particular the trailing edge of the spectrum, is sensitive to the W mass. Therefore, by fitting the experimental distribution of the transverse mass with Monte Carlo samples generated with different values of m_W, it is possible to obtain the mass which best fits the data. The trailing edge is smeared by several effects, such as the W intrinsic width and the detector resolution. This is illustrated in Figure 16-1, which shows the distribution of the W transverse mass as obtained at particle level (no detector resolution) and by including the energy and momentum resolution as implemented in ATLFAST. The smearing due to the finite resolution reduces the sharpness of the end-point and therefore the sensitivity to m_W.

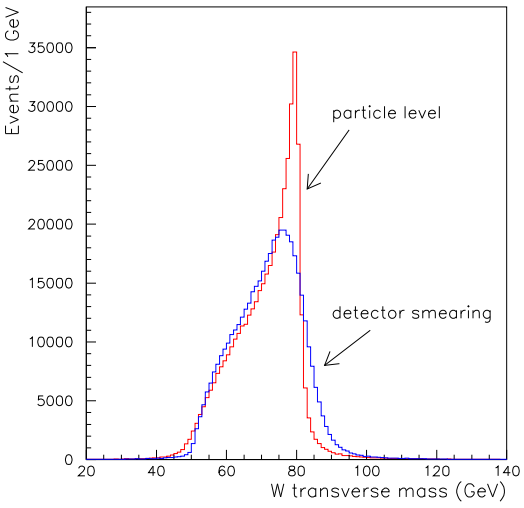

Figure 16-1 Distribution of the W transverse mass as obtained at particle level and by including the expected ATLAS detector resolution.

When running at high luminosity, the pile-up will smear significantly the transverse mass distribution, therefore the use of the transverse-mass method will probably be limited to the initial phase at low luminosity. Alternative methods are mentioned in Section 16.1.4.

16.1.2 *W* production and selection

At the LHC, the cross-section for the process $pp \rightarrow W+X$ with $W \rightarrow l\nu$ and $l = e, \mu$ is 30 nb. Therefore, about 300 million events are expected to be produced in one year of data taking at low luminosity. Such a cross-section is a factor of ten larger than at the Tevatron ($\sqrt{s}$ = 1.8 TeV).

To extract a clean *W* signal, one should require:

- An isolated charged lepton (e or μ) with $p_T > 25$ GeV inside the region devoted to precision physics $|\eta| < 2.4$.
- Missing transverse energy $E_T^{miss} > 25$ GeV.
- No jets in the event with $p_T > 30$ GeV.
- The recoil should satisfy $|\vec{u}| < 20$ GeV.

The last two cuts are applied to reject *W*'s produced with high p_T, since for large $p_T{}^W$ the transverse mass resolution deteriorates and the QCD background increases. The acceptance of the above cuts is about 25%. By assuming a lepton reconstruction efficiency of 90% and an identification efficiency of 80%, a total selection efficiency of about 20% should be achieved. Therefore, after all cuts about 60 million *W*'s are expected in one year of data taking at low luminosity (10 fb^{-1}), which is a factor of about 50 larger than the statistics expected from the Tevatron Run 2.

16.1.3 Expected uncertainties

Due to the large expected event sample, the statistical uncertainty on the *W* mass should be smaller than 2 MeV for an integrated luminosity of 10 fb^{-1}.

Since the *W* mass is obtained by fitting the experimental distribution of the transverse mass with Monte Carlo samples, the systematic uncertainty will come mainly from the Monte Carlo modelling of the data, *i.e.* the physics and the detector performance. Uncertainties related to the physics include the knowledge of: the *W* p_T spectrum and angular distribution, the parton distribution functions, the *W* width, the radiative decays and the background. Uncertainties related to the detector include the knowledge of: the lepton energy and momentum scale, the energy and momentum resolution, the detector response to the recoil and the effect of the lepton identification cuts. At the LHC, as now at the Tevatron, most of these uncertainties will be constrained *in situ* by using data samples such as $Z \rightarrow ll$ decays. The latter will be used to determine the lepton energy scale, to measure the detector resolution, to model the detector response to the *W* recoil and the p_T spectrum of the *W*, *etc.*

The advantages of ATLAS with respect to the Tevatron experiments are:

- The large number of *W* events mentioned above.
- The large size of the 'control samples'. About six million $Z \rightarrow ll$ decays, where $l = e, \mu$, are expected in one year of data taking at low luminosity after all selection cuts. This is a factor of about 50 larger than the event sample from the Tevatron Run 2.
- ATLAS is more powerful than CDF and D0 are, in terms of energy resolution, particle identification capability, geometrical acceptance and granularity. Maybe more important for this measurement is the fact that ATLAS will benefit, when data taking will start, from extensive and detailed simulation and test-beam studies of the detector performance.

Nevertheless, ATLAS is a complex detector, which will require a great deal of study before its behaviour is well understood [16-4].

To evaluate the expected systematic uncertainty on the W mass, $W \to l\nu$ decays were generated with PYTHIA and processed with ATLFAST. After applying the selection cuts discussed above, a transverse mass spectrum was produced for a reference mass value (80.300 GeV). All sources of systematic uncertainty affecting the measurement of the W mass from CDF Run 1A [16-5] were then considered (recent CDF and D0 results based on the full Run 1 statistics can be found in [16-6]). Their magnitude was evaluated in most cases by extrapolating from the Tevatron results, on the basis of the expected ATLAS detector performance. The resulting error on the W mass was determined by generating new W samples, each one including one source of uncertainty, and by comparing the resulting transverse mass distributions with the one obtained for the reference mass. A Kolmogorov test [16-7] was used to evaluate the compatibility between distributions.

Since the goal is a total error of ~20 MeV, the individual contributions should be much smaller than 10 MeV. A large number of events was needed to achieve such a sensitivity. With three million events after all cuts, corresponding to twelve million events at the generation level, a sensitivity at the level of 8 MeV was obtained.

The main sources of uncertainty and their impact on the W mass measurement are discussed one by one in the next Sections. The total error and some concluding remarks are presented in Section 16.1.4.

16.1.3.1 Lepton energy and momentum scale

This is the dominant source of uncertainty on the measurement of the W mass from Tevatron Run 1, where the absolute lepton scale is known with a precision of about 0.1% [16-5][16-8]. Most likely, this will be the dominant error also at the LHC. Indeed, in order to measure the W mass with a precision of 20 MeV or better, the lepton scale has to be known to 0.02%. The latter is the most stringent requirement on the energy and momentum scale from LHC physics. It should be noted that a precision of 0.04% must be achieved by the Tevatron experiments in Run 2, in order to measure the W mass to 40 MeV [16-2].

The lepton energy and momentum scale will be calibrated *in situ* at the LHC by using physics samples, which will complement the information coming from the hardware calibration and the test-beam measurements. The methods and preliminary results from full-simulation studies are discussed in Chapter 12. The muon scale will be calibrated by using mainly $Z \to \mu\mu$ events, and the EM Calorimeter scale will be calibrated by using mainly $Z \to ee$ events or E/p measurements for isolated electrons. The main advantage of the LHC compared to the Tevatron is the above-mentioned large sample of $Z \to ll$ decays. The Z boson is close in mass to the W boson, therefore the extrapolation error from the point where the scale is determined to the point where the measurement is performed is small. In Run 1A, due to the small number of Z events, the central tracker of CDF was calibrated by using $J/\psi \to \mu\mu$ decays, whereas the calorimeter scale was transferred from the tracker by using E/p measurements for isolated electrons [16-5]. The extrapolation error from the J/ψ mass to the W mass is one of the dominant sources of uncertainty in the CDF measurement of the W mass from Run 1A. For Run 1B [16-6], $J/\psi \to \mu\mu$ and $\Upsilon \to \mu\mu$ decays were used as cross-checks, but $Z \to \mu\mu$ was used as the reference mass to determine the momentum scale, thanks to the larger statistics compared to Run 1A. For what concerns the energy scale, inconsistencies in the E/p scale determination have not been resolved, therefore the

calorimeter scale is based solely on the $Z \rightarrow ee$ mass. In the absence of a magnetic field, D0 can only use $Z \rightarrow ee$ events to calibrate the EM Calorimeter [16-8]. The resulting uncertainty is dominated by the limited statistics of the Z sample.

The error on the absolute lepton scale to be expected in ATLAS was evaluated by extrapolating from the CDF uncertainties for Run 1A. It was found that, both for electrons and muons, an uncertainty of 0.02% is difficult to achieve but not impossible. This has been confirmed by full-simulation studies (Chapter 12). To reach such a precision, however, several experimental constraints, *e.g.* knowledge of the magnetic field to the 0.1% level [1] and of the Inner Detector material to ~1%, should be satisfied. Indeed, only in an overconstrained situation will it be possible to disentangle the various contributions to the detector response, and therefore to derive a reliable systematic error.

16.1.3.2 Lepton energy and momentum resolution

To limit the uncertainty on the W mass from the lepton resolution to less than 10 MeV, the EM Calorimeter energy resolution and the Inner Detector and Muon System momentum resolutions have to be known with a precision of better than 1.5%.

The lepton energy and momentum resolution will be determined at the LHC by using information from test-beam and from Monte Carlo simulations of the detector, as well as *in situ* measurement of the Z width in $Z \rightarrow ll$ final states. These methods are used presently at the Tevatron. As an example, the statistical error on the momentum resolution obtained by CDF in Run 1A is 10%, whereas the systematic error is only 1% and is dominated by the uncertainty on the radiative decays of the Z [16-5]. Since the performance of the ATLAS Inner Detector in terms of momentum resolution is expected to be similar to that of CDF, and since the statistical error at the LHC will be negligible, a total error of less than 1.5% should be achieved. There is even the possibility that this uncertainty decreases, if improved theoretical calculations of radiative Z decays will become available.

16.1.3.3 W p_T spectrum

The modelling of ${p_T}^W$ in the Monte Carlo is affected by both theoretical and experimental uncertainties. Theoretical uncertainties arise from the difficulty in predicting the non-perturbative regime of soft-gluon emission, as well as from missing higher-order QCD corrections (see Section 15.7.3). Experimental uncertainties are mainly related to the difficulty of simulating the detector response to low-energy particles.

Therefore, the method used by CDF to obtain a reliable estimate of ${p_T}^W$ for Run 1A consisted of measuring the p_T distribution of the Z boson from $Z \rightarrow ll$ events in the data, and using the ${p_T}^Z$ spectrum as an approximation for the ${p_T}^W$ spectrum in the Monte Carlo, exploiting the fact that both gauge bosons have similar p_T distributions. The ${p_T}^W$ distribution obtained in this way can be further improved by requiring that the recoil distributions in the Monte Carlo and in the W data agree [16-5]. The resulting error on the W mass from CDF Run 1A is about 45 MeV per channel and is dominated by the limited statistics of the Z and W samples in the data [16-5]. For

1. In order to meet this requirement, one month during detector installation will be devoted to the measurement of the magnetic field.

Run 1B an improved method was adopted, which consisted of using the theoretical prediction for the ratio $p_T{}^W/p_T{}^Z$ (in this ratio several uncertainties cancel) to convert the measured $p_T{}^Z$ into $p_T{}^W$.

At the LHC, the average transverse momentum of the W (Z) is 12 GeV (14 GeV), as given by PYTHIA. Over the range p_T (W,Z) < 20 GeV, both gauge bosons have p_T spectra which agree to within ±10%. By assuming a negligible statistical error on the knowledge of $p_T{}^Z$, which will be measured with high-statistics data samples, and by using the $p_T{}^Z$ spectrum instead of the $p_T{}^W$ distribution, an error on the W mass of about 10 MeV per channel was obtained without any further tuning. Although the leading-order parton shower approach of PYTHIA is only an approximation to reality (see Section 15.7.3), this result is encouraging. Furthermore, improved theoretical calculations for the ratio of the W and Z p_T should become available at the time of the LHC, so that the final uncertainty will most likely be smaller than 10 MeV.

16.1.3.4 Recoil modelling

The transverse momentum of the system recoiling against the W, together with the lepton transverse momentum, is used to determine the p_T of the neutrino (see Equation 16-1). The recoil is mainly composed of soft hadrons from the underlying event, for which neither the physics nor the detector response are known with enough accuracy. Therefore, in order to get a reliable recoil distribution in the Monte Carlo, information from data is used at the Tevatron, and will most likely be used also at the LHC. More precisely, in each Monte Carlo event with a given $p_T{}^W$, the recoil is replaced by the recoil measured in the data for Z events characterised by a p_T of the Z boson similar to the above-mentioned $p_T{}^W$. The resulting error on the W mass from CDF Run 1A is 60 MeV per channel, and is dominated by the limited statistics of Z data. Results from CDF and D0 based on the full statistics of Run 1[16-6] show that this uncertainty scales with $\sqrt{N}$, where N is the number of events. Extrapolating to the LHC data sample, an error of smaller than 10 MeV per channel should be achieved. It should be noted that the recoil includes the contribution of the pile-up expected at low luminosity (two minimum-bias events per bunch crossing on average).

16.1.3.5 *W* width

The intrinsic width of the W, which is known with a precision of 85 MeV from measurements at the Tevatron, translated into an error of 20 MeV per channel on the W mass measurement from CDF Run 1A [16-5].

At hadron colliders, the W width can be obtained from the measurement of R, the ratio between the rate of leptonically decaying W's and leptonically decaying Z's:

$$R = \frac{\sigma_W}{\sigma_Z} \times \frac{BR(W \to l\nu)}{BR(Z \to ll)}$$

where the Z branching ratio (BR) is obtained from LEP measurements, and the ratio between the W and the Z cross-sections is obtained from theory. By measuring R, the leptonic branching ratio of the W can be extracted from the above formula, and therefore Γ_W can be deduced assuming Standard Model couplings for the W. The precision achievable with this method is limited by the theoretical knowledge of the ratio of the W to the Z cross-sections. Another method consists of fitting the high-mass tails of the transverse mass distribution, which are sensitive to the W width.

At the Tevatron Run 2 the *W* width should be measured with a precision of 30 MeV by using both the above-mentioned methods [16-2], which translates into an error of 7 MeV per channel on the *W* mass. This is however a conservative estimate for the LHC, since one could also use the *W* width as predicted by the Standard Model, as it has been done by CDF for Run 1B. Furthermore, the *W* width should be measured at the LHC with high precision by using the high-mass tails of the transverse mass distribution, as mentioned above.

16.1.3.6 Radiative decays

Radiative $W \to l\nu\gamma$ decays produce a shift in the reconstructed transverse mass, which must be precisely modelled in the Monte Carlo. Uncertainties arise from missing higher-order corrections, which translated into an error of 20 MeV on the *W* mass as measured by CDF in Run 1A. Improved theoretical calculations have become available since then [16-9]. Furthermore, the excellent granularity of the ATLAS EM Calorimeter, and the large statistics of radiative Z decays (Section 12.3.2), should provide useful additional information. Therefore, a *W* mass error of 10 MeV per channel was assumed in this study.

16.1.3.7 Background

Backgrounds distort the *W* transverse mass distribution, contributing mainly to the low-mass region. Therefore, uncertainties on the knowledge of the background rate and shape translate into an error on the *W* mass. This error is at the level of 10 MeV (25 MeV) in the electron (muon) channel for the measurement performed by CDF in Run 1A, where the background was known with a precision of about 15% [16-5].

A study was made of the main backgrounds to $W \to l\nu$ final states to be expected in ATLAS. The contribution from $W \to \tau\nu$ decays should be of order 1.3% in both, the electron and the muon channel. The background from $Z \to ee$ decays to the $W \to e\nu$ channel is expected to be negligible, whereas the contribution of $Z \to \mu\mu$ decays to the $W \to \mu\nu$ channel could amount to 4%. The difference between these two channels is due to the fact that the Calorimetry coverage extends up to $|\eta| \sim 5$, whereas the coverage of the Muon System is limited to $|\eta| < 2.7$. Therefore, muons from Z decays which are produced with $|\eta| > 2.7$ escape detection and thus give rise to a relatively large missing transverse momentum. On the other hand, electrons from Z decays produced with $|\eta| > 2.4$ are not efficiently identified, because of the absence of tracking devices and of fine-grained Calorimetry, however their energy can be measured up to $|\eta| \sim 5$. Therefore these events do not pass the E_T^{miss} cut described in Section 16.1.2. Finally, $t\bar{t}$ production and QCD processes are expected to give negligible contributions.

In order to limit the error on the *W* mass to less than 10 MeV, the background to the electron channel should be known with a precision of 30%, which is easily achievable, and the background to the muon channel should be known with a precision of 7%. The latter could be monitored by using $Z \to ee$ decays.

16.1.4 Results

The expected contributions to the uncertainty on the *W* mass measurement, of which some are discussed in the previous Sections, are presented in Table 16-1. With an integrated luminosity of 10 fb^{-1}, and by considering only one lepton species (*e* or μ), the total uncertainty should be about 25 MeV. By combining both lepton channels, which should also provide useful cross-checks

since some of the systematic uncertainties are different for the electron and the muon sample, an error of about 20 MeV should be achieved by ATLAS alone. This error should decrease to about 15 MeV by combining ATLAS and CMS together. Such a precision would allow the LHC to compete with the expected precision at a Next Linear Collider [16-10].

The most serious challenge in this measurement is the determination of the lepton absolute energy and momentum scale to 0.02%. All other uncertainties are expected to be of the order of (or smaller than) 10 MeV. Preliminary results from CDF including the full statistics from Run 1 [16-6] indicate that many of the errors in the second column of Table 16-1 have indeed approached the ATLAS expected uncertainties given in the third column. For instance, the present CDF error coming from uncertainties in the parton distribution functions is only 15 MeV.

To achieve such a goal, improved theoretical calculations of radiative decays, of the W and Z p_T spectra, and of higher-order QCD corrections will be needed.

The results presented here have to be considered as preliminary and far from being complete. It may be possible that, by applying stronger selection cuts, for instance on the maximum transverse momentum of the W, the systematic uncertainties may be reduced further. Moreover, two alternative methods to measure the W mass can be envisaged. The first one uses the p_T distribution of the charged lepton in the final state. Such a distribution features a Jacobian peak at

Table 16-1 Expected contributions to the uncertainty on the W mass measurement in ATLAS for each lepton family and for an integrated luminosity of 10 fb^{-1} (third column). The corresponding uncertainties of the CDF measurement in the electron channel, as obtained in Run 1A [16-5], are also shown for comparison (second column).

Source	Δm_W (CDF)	Δm_W (ATLAS)
Statistics	145 MeV	< 2 MeV
E-p scale	120 MeV	15 MeV
Energy resolution	80 MeV	5 MeV
Lepton identification	25 MeV	5 MeV
Recoil model	60 MeV	5 MeV
W width	20 MeV	7 MeV
Parton distribution functions	50 MeV	10 MeV
Radiative decays	20 MeV	< 10 MeV
${p_T}^W$	45 MeV	5 MeV
Background	10 MeV	5 MeV
TOTAL	230 MeV	25 MeV

$p_T^l \sim m_W/2$ and has the advantage of being affected very little by the pile-up, therefore it could be used at high luminosity. However, the lepton momentum is very sensitive to the p_T of the W boson, whereas the transverse mass is not, and hence a precise theoretical knowledge of the W p_T spectrum would be needed to use this method. Another possibility is to use the ratio of the transverse masses of the W and Z bosons [16-11]. The Z transverse mass can be reconstructed by using the p_T of one of the charged leptons, whilst the second lepton is treated like a neutrino

whose p_T is measured by the first lepton and the recoil. By shifting the m_T^Z distribution until it fits the m_T^W distribution, it is possible to obtain a scaling factor between the W and the Z mass and therefore the W mass. The advantage of this method is that common systematic uncertainties cancel in the ratio. The main disadvantage is the loss of a factor of ten in statistics, since the $Z \to ll$ sample is a factor of ten smaller than the $W \to l\nu$ sample. Furthermore, differences in the production mechanism between the W and the Z (p_T, angular distribution, *etc.*), and possible biasses coming from the Z selection cuts, will give rise to a non-negligible systematic error.

The final measurement will require using all the methods discussed above, in order to cross-check the systematic uncertainties and to achieve the highest precision.

16.2 Gauge-boson pair production

The principle of gauge invariance is used as the basis for the Standard Model. The non-Abelian gauge-group structure of the theory of Electroweak Interactions predicts very specific couplings between the Electroweak gauge bosons. Measurements of these Triple Gauge-boson Couplings (TGC) and Quadruple Gauge-boson Couplings (QGC) of the W, Z and γ gauge-bosons provide powerful tests of the Standard Model.

Any theory predicting physics beyond the Standard Model, while maintaining the Standard Model as a low-energy limit, may introduce deviations in the couplings. Precise measurements of the couplings will not only be a stringent test of the Standard Model and the electro-weak symmetry breaking, but also probe for new physics in the bosonic sector, and will provide complementary information that given by direct searches for new physics. Radiative corrections within the Standard Model also introduce small deviations in the values of the couplings from those expected at lowest order. The deviations are typically of order of O(0.001); deviations due to corrections from supersymmetric or technicolour theories are comparable to this [16-12]. Experiments that can reach this sensitivity could provide powerful constraints on these models.

In the most general Lorentz invariant parametrisation, the three gauge-boson vertices, $WW\gamma$ and WWZ, can be described by fourteen independent couplings [16-13], seven for each vertex. The possible four quadruple gauge-boson vertices: $\gamma\gamma WW$, $Z\gamma WW$, $ZZWW$ and $WWWW$ require 36, 54, 81 and 81 couplings, respectively for a general description. However, on very general theoretical grounds [16-14], it is not possible to introduce QGCs which would not affect the TGCs. In view of this the study presented here concentrate on the TGCs.

Assuming electromagnetic gauge invariance, C- and P-conservation, the set of 14 couplings for the three gauge-boson vertices is reduced to 5: g_1^Z, κ_γ, κ_Z, λ_γ and λ_Z [16-15], where their Standard Model values are equal to $g_1^Z = \kappa_\gamma = \kappa_Z = 1$ and $\lambda_\gamma = \lambda_Z = 0$ at tree level.

The TGCs related to the $WW\gamma$ vertex determine properties of the W, such as its magnetic dipole moment μ_W and electric quadrupole moment q_W:

$$\mu_W = \frac{e}{2m_W}(g_1^Z + \kappa_\gamma + \lambda_\gamma)$$

$$q_W = \frac{e}{m_W^2}(\kappa_\gamma - \lambda_\gamma)$$

In the following the TGCs are denoted Δg_1^Z, $\Delta\kappa_\gamma$, $\Delta\kappa_Z$, λ_γ and λ_Z, where the Δ denotes the deviations of the respective quantity from its Standard Model value.

The values of the TGCs in the Standard Model are such that scattering processes involving gauge bosons at high energy respect unitarity. Modification of the couplings leads to a potential violation of unitarity since the effective parametrisation does not provide the cancellations at very high energies occur in the Standard Model. To restore unitarity at high energies the TGCs are modified by a dipole form factor with a scale Λ, such that $TGC \rightarrow TGC/(1+s/\Lambda^2)^2$, where $\sqrt{s}$ is the centre-of-mass energy of the hard scattering process. Unless otherwise stated, the scale, Λ, is 10 TeV in the study presented here, corresponding to the point where the unitarity limit and the experimental precision are comparable.

The current limits on the TGCs obtained from the combined Tevatron and LEP2 measurements range from O(0.1) for $\Delta\kappa_\gamma$ to O(0.01) for λ_γ. Extrapolating to the year 2005 leads one to expect that these limits will improve by a a factor 10.

The measurement of the TGCs presented here concentrates on fully leptonic final states of $W\gamma$ and WZ production. Backgrounds are expected to be higher in the WW channel and in final states involving jets.

16.2.1 $W\gamma$ Production

The characteristic features of leptonic final states of $W\gamma$ di-boson events, that is, $W\gamma \rightarrow l\nu\gamma$ where $l = e$ or μ, imply that extraction of the signal should be straightforward as it involves a high p_T lepton and γ in connection with large missing p_T. On the other hand, the expected signal cross section is small, about 350 fb for $p_T^\gamma > 100$ GeV; several orders of magnitude below the dominant heavy flavour production processes of QCD that can also lead to events with isolated leptons and large missing energy. The background can be split in one set of events with prompt leptons and γ's and another set of events where one or more jets have been mis-identified as leptons or γ's. Both sets have their main contribution from heavy flavour pair production, $b\bar{b}$ and $t\bar{t}$, with possible hard QED γ's. Additional contributions to the latter set of events come from prompt γ production, $q\gamma$, and W production. The following selection is made [16-16].

- Only one γ with high p_T ($p_T > 100$ GeV);
- Only one high p_T lepton ($p_T > 40$ GeV) (efficiency of 90% has been assumed);
- Both the lepton and the γ should be isolated, $E_{cone} < 12$ GeV for a cone of radius 0.2;
- Large transverse mass of the lepton and missing p_T system, $m_T^W > 35$ GeV;
- No remaining large jet activity, $E_{T,max}(\text{jet}) < 20$ GeV.

These requirements bring the background down to about 20% of the signal, and reduce the expected number of events for an integrated luminosity of 30 fb^{-1} to slightly less than 3000. The very efficient mis-identification rejection in ATLAS (see Sections 7.4, 7.6 and 7.7) implies that the dominant background comes from events with prompt leptons and γ's which populate the lower end of the p_T spectrum. In contrast, the contribution from events with high-p_T jets mis-identified as leptons or γ is much smaller, but their p_T range is larger.

16.2.1.1 Kinematic reconstruction

In purely leptonic final states from $W\gamma$ di-boson events the momentum of the neutrino can be reconstructed by using the W mass as a constraint and assuming that the missing transverse energy is carried off by the neutrino. There is a a two-fold ambiguity in this reconstruction. In the following all distributions that depend explicitly on the neutrino momentum have two entries with equal weight corresponding to this ambiguity. The finite W width is not included in the reconstruction hypothesis and there exist events without a physical solution. For the majority of these events a unique solution is found by neglecting the imaginary part of the complex solution, corresponding to a minimal change of the W mass hypothesis in order to obtain a physical solution.

16.2.2 *WZ* Production

In analogy with the $W\gamma$ analysis, only leptonic final states from WZ production, $WZ \rightarrow lll\nu$, where $l = e$ or μ, have been studied. The signal cross section of WZ production is approximately 26 pb at the LHC, reducing to almost 95 fb for $p_T^Z > 100$ GeV. Fully leptonic final states from WZ production are identified by having three energetic leptons, of which two are of equal flavour and opposite charge, in addition to missing p_T. As in $W\gamma$ production case, the dominant background sources are heavy flavour pair production; additional contributions from prompt $Z\gamma$ and Z production with jet mis-identification also contribute. These can be reduced by requiring [16-16]

- Exactly three high p_T leptons ($p_T > 25$ GeV);
- At least one pair of leptons should have same flavour and opposite sign and have an invariant mass consistent with that of a Z, $|m_{ll}\text{-}m_Z| > 10$ GeV;
- Large transverse mass of the lepton and missing p_T system, $m_T^W > 40$ GeV;
- No remaining large jet or γ activity, $p_T^\gamma < 50$ GeV and $E_{T,max}(\text{jet}) < 20$ GeV.

After this selection, about 1200 events remain with a purity of approximately 70% for an integrated luminosity of 30 fb^{-1}.

The reconstruction of the WZ event kinematics follows the same procedure as for the $W\gamma$ reconstruction (Section 16.2.1.1).

16.2.3 Determination of Triple Gauge Couplings

The experimental sensitivity to the TGCs comes from the increase of the production cross section and the alteration of differential distributions for non-standard TGCs. The sensitivity is further enhanced at high centre-of-mass energies of the hard scattering process; This effect is more significant for λ type TGCs than for κ type TGCs. As a consequence an increase of in the number of events with large di-boson invariant masses is a clear signature of non-standard TGCs as illustrated on Figure 16-2, where the invariant mass of the hard scattering is shown for $W\gamma$ events simulated with the ATLFAST detector simulation program for the Standard Model and non-standard TGCs. For non-standard values of the TGCs the simulation of the hard scattering is based on a leading order calculation [16-15]. In this way, limits on the TGCs can be obtained from event counting in the high-mass region. The disadvantage of such an approach alone is that the behaviour of the cross section as function of the TGCs is such that the ability to disen-

tangle the contributions from different TGCs and even their sign (with respect to SM) is poor. It is therefore advantageous to combine it with information from angular distributions, including the boson decay angles; this improves the sensitivity and enables the f the contributions from non-standard TGCs to be separated.

One observable, p_T of the γ or Z, traditionally used at hadron colliders, has sensitivity from a combination of high mass event counting and angular distributions. The enhanced sensitivity to the TGCs is due to the vanishing of helicity amplitudes in the Standard Model prediction at small $|\eta|$ [16-15]. Non-standard TGCs may partially eliminate this 'zero radiation', although the zero radiation prediction is less significant when including NLO corrections. Several variables and combinations thereof have been studied to assess the possible sensitivity to the TGCs. For both $W\gamma$ and WZ events the variables are very similar; the γ momentum is simply replaced with that of the Z reconstructed from the two leptons. The actual behaviour of the variables as function of the couplings and the energy is slightly different for the two processes, due to the mass of the Z. In this study two sets of variables have been used (and the equivalent set for WZ): ($m_{W\gamma}$, $|\eta_\gamma^*|$), and (p_T^γ, θ^*), where $|\eta_\gamma^*|$ is the rapidity of the γ with respect to the beam direction in the $W\gamma$ system, and θ^* is the polar decay angle of the charged lepton in the W rest-frame. Both sets consist of one variable sensitive to the energy behaviour and one sensitive to the angular information.

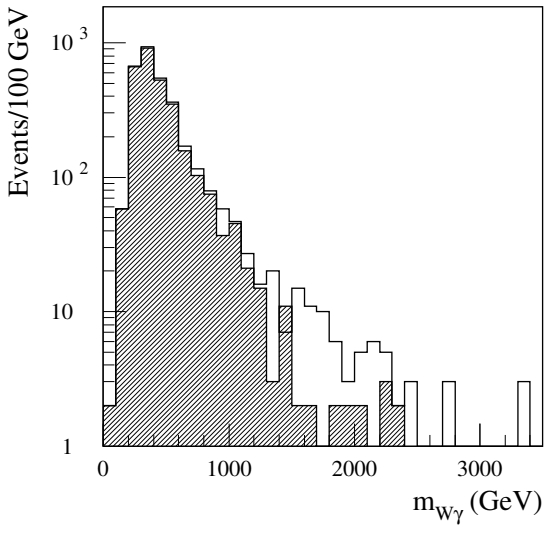

Figure 16-2 The distribution of the invariant mass of the $W\gamma$ system for the Standard Model (shaded histogram) and a non-standard value of 0.01 for $\lambda\gamma$ (white histogram). The number of events corresponds to an integrated luminosity of 30 fb^{-1}.

In principle, it possible is to reconstruct the four (six) variables for a $W\gamma$ (WZ) event, but lack of statistics make multidimensional binned fits using all information difficult. Alternatively, probability distributions can be constructed by integrating over the initial parton configuration using Monte Carlo.

Distributions of some of the variables used in this analysis are shown in Figures 16-3 and 16-4, for both the standard model expectation and different non-standard TGCs. The strong enhancement for non-standard TGCs at high p_T is clearly visible and, furthermore, the qualitative behaviour is the same for different TGCs. The high sensitivity to the TGCs from $|\eta_\gamma^*|$ is due to the characteristic 'zero radiation' gap. In contrast the sensitivity to the TGCs from the decay polar angle, θ^* is weak; it primarily serve as a projector of different helicity components and thereby enhances the sensitivity from other variables.

The determination of the couplings from the different event channels studied in this analysis is done by binned maximum-likelihood fits to distributions of the variables, combined with the total cross-section information. The likelihood function is constructed by comparing the fitted histogram with a reference histogram using Poisson probabilities. The reference distributions are obtained for different values of the couplings by reweighting at generator level.

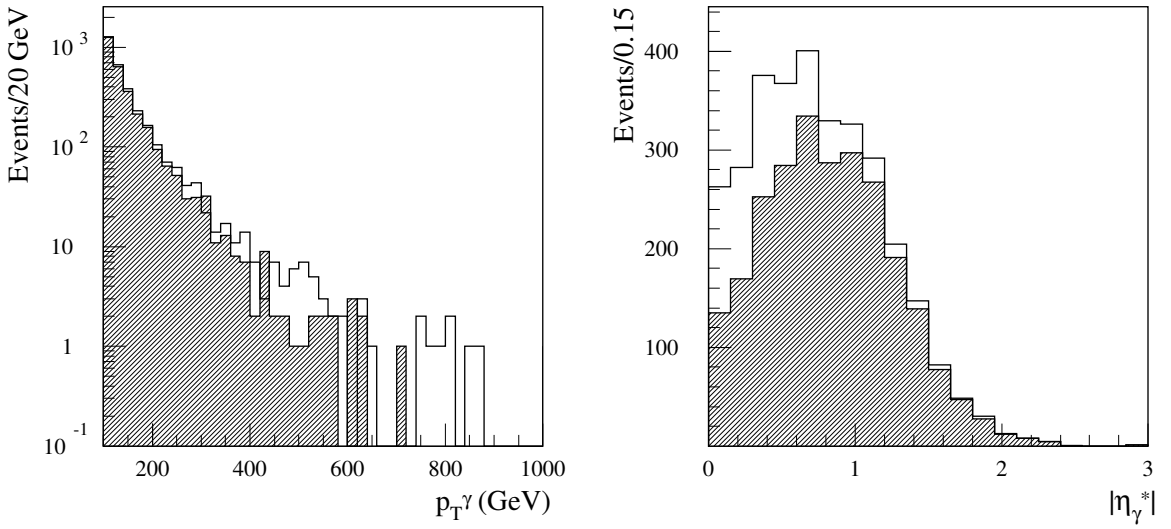

Figure 16-3 Distribution of p_T^γ (left) and $|\eta_\gamma^*|$ (right) from $W\gamma$ events for an integrated luminosity of 30 fb^{-1}. Distributions are shown for the Standard Model (shaded histograms) and for non-standard values (white histograms) $\lambda_\gamma = 0.01$ (left) and $\Delta\kappa_\gamma = 0.2$ (right).

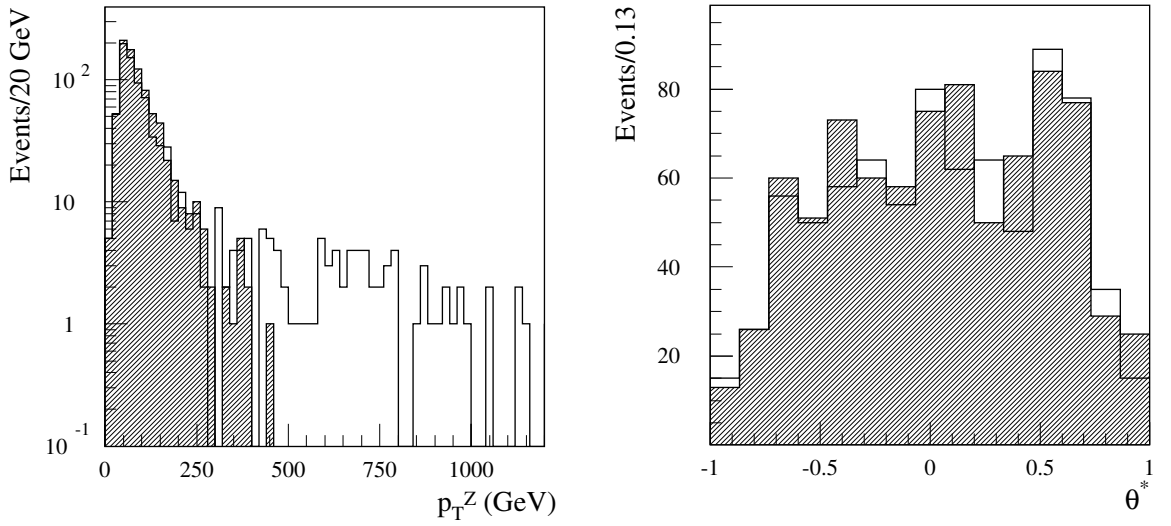

Figure 16-4 Distribution of p_T^Z (left) and θ^* (right) from WZ events for an integrated luminosity of 30 fb^{-1}. Distributions are shown for the Standard Model (shaded histograms) and for non-standard values (white histograms) $\Delta g_1^Z = 0.05$ (left) and $\Delta\kappa_Z = 0.2$ (right).

16.2.4 Systematic uncertainties

At the LHC, the sensitivity to the TGCs is a combination of the very high energy and high luminosity. As the main sensitivity is given by the very high end of the p_T distributions, the important sources of systematic error are those which affect the high energy spectrum. Consequently, the uncertainty arising from the imprecise knowledge of the background is expected to be quite small in the measurement of the TGCs as the dominant background is concentrated at low p_T;

non-standard TGCs would increase the number of events in the high end of the p_T spectrum. For example, the precision on λ_γ was estimated for a sample with a tighter cut on p_T^γ (>200 GeV). The corresponding change in sensitivity is less than 1%, despite a reduction by more than a factor 10 in the total number of signal events. In the case of $\Delta\kappa_\gamma$ the change in sensitivity is larger; about 50%. The reason for this difference between λ-type and κ-type TGCs is that the precision on λ-type TGCs arises from the high energy behaviour, whereas the limits on the κ-type TGCs benefit from angular information, and, hence, are statistically limited.

Of more theoretical oriented uncertainties to the p_T distribution is the choice of pdf and higher order corrections. Higher order corrections have been calculated [16-17] and give substantial contributions, up to a factor 3 (Section 15.7.5), and also alter the differential distributions leading to a loss in precision, with the possibility of mimicking non-standard TGCs if not properly accounted for in the fit to data [16-17]. The combination of all these effects will manifest themselves to lowest order as uncertainties in the a p_T scale.

Finally, it should be stressed that not all observables are equally susceptible to systematic uncertainties. The requirement of a complete reconstruction of the event kinematics introduces many additional sources of systematic errors as it can be seen from the *W* mass measurement (Section 16.1.2), favouring the more robust measurement of distributions of p_T of either γ or *Z*, where the exact knowledge of the W kinematics is less important.

16.2.5 Results

The expected 95% C.L. limits on the TGCs obtained from fits to binned distributions of observables are listed in Table 16-2 for fits where one coupling is allowed to vary at the time, with the other couplings held fixed at their Standard Model values. For comparison, the ideal case with maximal sensitivity using an unbinned fit to the complete 6 (8) dimensional phase- space distribution of *W*γ (*WZ*) production at generator level is also shown. Such a method relies on the complete reconstruction of the event including the knowledge of the initial partonic configuration and will not be applicable to data. From Table 16-2 it is clear that a part of the sensitivity to the κ type TGCs come from the angular information, whereas sensitivity to the λ type TGCs is completely dominated by the very high energy tails.

Table 16-2 The envisaged statistical precision from single parameter fits for a given coupling, assuming an integrated luminosity of 30 fb^{-1}. The limits are presented for the different sets of variables and the ideal case denote fits at generator level using all available information.

Coupling	95% C.L. ($m_{W\gamma}$, $\lvert\eta^*\rvert$)	95%C.L. (p_T^γ, θ^*)	95%C.L. Ideal case
$\Delta\kappa_\gamma$	0.035	0.046	0.028
λ_γ	0.0025	0.0027	0.0023
Δg_1^Z	0.0078	0.0089	0.0053
$\Delta\kappa_Z$	0.069	0.100	0.058
λ_Z	0.0058	0.0071	0.0055

The single parameter limits shown in Table 16-2 represent the best possible precision in the search for anomalous TGCs. In the case of non-standard TGCs, a general multiparameter fit is the only way to establish the nature of the non-standard contribution. For the *WW*γ TGCs the correlation between $\Delta\kappa_\gamma$ and λ_γ is small and the two parameter limits are close to the limits in Table 16-2. In contrast the correlation between Δg_1^Z and $\Delta\kappa_Z$ is quite large (~50%) worsening the general three parameter limits with about 25%.

In summary a precision of O(0.001) for the best constrained couplings, comparable to the world-limit at the time of the LHC start-up, can be achieved with only 10 fb^{-1} corresponding to one year of running at low luminosity.

16.3 Conclusions

Preliminary studies indicate that measuring the *W* mass with a precision of about 20 MeV will be challenging. The biggest single advantage of the LHC is the large statistics, which will permit small statistical errors and good control of the systematic uncertainties.

The study of gauge boson pair production in the first years of the LHC will provide a unique opportunity to perform high precision measurements, which will put stringent constraints on the electroweak symmetry breaking and the gauge group structure of the Standard Model, well beyond the precision at the time of the LHC start-up.

To achieve such unprecedented precision, improved theoretical calculations in many areas will be needed, and several challenging experimental requirements will have to be satisfied.

16.4 References

16-1 G. Altarelli, T. Sjöstrand and F. Zwirner, 'Physics at LEP2', CERN 96-01 (1996).

16-2 D. Amidei and R. Brock, 'Future electroweak physics at the Fermilab Tevatron', FERMILAB-PUB-96/082 (1996).

16-3 F. Gianotti, 'Measurement of the *W* mass at the LHC', ATLAS Internal Note ATL-COM-PHYS-99-063 (1999).

16-4 S. Haywood, 'Offline calibration and alignment of the Inner Detector', ATLAS Internal Note ATL-INDET-99-001 (1999).

16-5 CDF Collaboration, Phys. Rev. **D 52** (1995) 4784.

16-6 M. Lancaster, 'New results on W mass', talk given at the XXXIV Rencontres de Moriond, March 1999, Les Arcs, France.

16-7 Eadie *et al.*, 'Statistical methods in experimental physics', North-Holland, (1971) 269.

16-8 D0 Collaboration, Phys. Rev. Letters **80** (1998) 3008.

16-9 U. Baur *et al.*, Phys. Rev. **D56** (1997) 140.

16-10 E. Accomando *et al.*, 'Physics with e^+e^- Linear Colliders', DESY 97-100, hep-ph/9705442 (1997).

16-11 S. Rajagopalan and M. Rijssenbeek, 'Measurement of m_W using the transverse mass ratio of *W* and *Z*', in Proceedings of the Workshop on New Directions in High Energy Physics, Snowmass 1996.

16-12 J. Ellison and J. Wudka, Ann. Rev. Nucl. Part. Sci. **48** (1998) 33.

16-13 K.Hagiwara, R.Peccei, D. Zeppenfeld and K.Hikasa, Nucl. Phys. **B282** (1987) 253.

16-14 D. Zeppenfeld, private communication.

16-15 U. Baur and D. Zeppenfeld, Nucl. Phys. **B308** (1988) 127.

16-16 D. Fouchez, 'Gauge bosons pair production study with ATLAS', ATLAS Internal Note ATL-PHYS-NO-060 (1994).

16-17 U. Baur, T. Han and J. Ohnemus, Phys. Rev. **D48** (1993) 5140; Phys. Rev. **D51** (1995) 3381.